# Metal $\pi$ Complexes of Benzene Derivatives. 44.[1] The (-PMe)$_2$Co$_2$(CO)$_4$(PMe$_2$-)$_2$ Unit as a Spacer between Bis($\eta$-arene)metal Pairs (M = V, Cr). Electrochemical and EPR Spectroscopic Study of Interactions within the Tetranuclear Complexes

Christoph Elschenbroich,* Bernhard Metz, and Bernhard Neumüller

*Fachbereich Chemie, Philipps-Universität, D-35032 Marburg, Germany*

Edward Reijerse

*Department of Molecular Spectroscopy, University of Nijmegen, 626 ED Nijmegen, The Netherlands*

*Received May 5, 1994*[⊗]

In order to study long-distance intermetallic communication between bis(arene)metals, we have synthesized the binuclear complexes [(Me$_2$P-$\eta^6$-C$_6$H$_5$)$_2$M]$_2$Co$_2$($\mu$-CO)$_2$(CO)$_2$ (**14**, M = V; **15**, M = Cr) in which the sandwich units are separated by the (-Me$_2$P)$_2$Co$_2$(CO)$_4$(P-Me$_2$-)$_2$ spacer. **14** crystallizes in the monoclinic space group $P2_1/c$, $Z = 4$, $a = 1465.2(3)$, $b = 1696.5(3)$, $c = 1571.1(3)$ pm, $\beta = 112.92(2)°$, $R = 5.8\%$. The axes of the two terminal sandwich units are twisted by an angle of 55.3°; the bending of the individual sandwich axes is small (4°). The distance between the terminal vanadium atoms amounts to 1094.2(3) pm. According to $^1$H-, $^{13}$C-, and $^{31}$P-NMR, the dichromium analog **15** in solution is fluxional for $173 < T < 295$ K due to an exchange process between terminal and bridging CO ligands and rapid chain reversals of the $-Me_2P-Co-PMe_2-$ interannular links. As revealed by cyclic voltammetry, the two tetranuclear complexes **14** and **15**, despite the large intermetallic distance, display a small redox splitting between successive oxidations of the terminal bis(arene) metal units. Intermetallic communication also manifests itself in the $^{51}$V hyperfine structure of the EPR spectrum of the biradical **14**$^{\bullet\bullet}$ in fluid solution, the analysis of which yields an exchange coupling constant of $J = -0.078$ cm$^{-1}$. Thus, for **14**$^{\bullet\bullet}$ an intermediate exchange situation obtains for which exchange coupling $J$ and hyperfine coupling $a(^{51}V)$ are of similar magnitude. For the isoelectronic species **15**$^{\bullet\bullet 2+}$, evidence characterizing its biradical nature is only obtainable from the rigid solution EPR spectrum of **15**(PF$_6$)$_2$, which exhibits a $\Delta M_s = 2$ signal and a trace in the $\Delta M_s = 1$ region from which a zero-field splitting parameter of $D = 26 \times 10^{-4}$ cm$^{-1}$ is estimated. If this value is used to calculate the interchromium distance, assuming that the point-dipole approximation is valid, the result falls short of the distance obtained from single-crystal X-ray analysis by 8%.

One of the incentives to prepare paramagnetic dinuclear complexes derives from the continuing interest in exploring how rapidly magnetic exchange interactions fall off as the bridging groups are made more extended.[2] There is ample evidence, however, that the extent of magnetic exchange does not display a simple dependence on intermetallic distance. This is because the superexchange and the magnetic dipole interaction possess different dependences on interspin separation, and in the region of about 8–14 Å they may be of comparable magnitude.[3] Consequently, the procedure for dipolar distance estimation in the presence of isotropic exchange interaction may furnish incorrect results. We have initiated a research program dealing with the synthesis and structural characterization of bis($\eta^6$-arene)metal(d$^5$) pairs separated by organometallic spacers like (-PMe$_2$)$_2$M′(PMe$_2$-)$_2$, M′ = Ni,[4a] Pt, CoH,[4b] and >Si(Ph)-Si(Ph)< (Chart 1).[5]

A prominent feature of complex 7$^{\bullet\bullet}$ is electron–electron spin–spin coupling over a distance of 760 pm, a Si–Si $\sigma$ bond serving as the propagating medium. The $^{51}$V hyperfine structure for 7$^{\bullet\bullet}$ denotes the fast-exchange case [$J \gg a(^{51}V)$], and in fact, spectral simulation leads to $J = -0.48 \pm 0.2$ cm$^{-1}$, which is to be compared with $a(^{51}V, \mathbf{7}) = 0.63 \times 10^{-2}$ cm$^{-1}$.[5] It was therefore of interest to explore the extent to which spin exchange would be weakened by introducing a larger spacer, by twisting the axes of the two communicating bis(arene)-metal units and by replacing the intraspacer Si–Si bond by a $\sigma$ bond between two transition metal atoms. These requirements are fullfilled by the spacer (-PMe$_2$)$_2$Co-(CO)$_2$Co(CO)$_2$(PMe$_2$-)$_2$, which is the subject of this paper.

⊗ Abstract published in *Advance ACS Abstracts,* November 1, 1994.

(1) Part 43: Elschenbroich, Ch.; Isenburg, T.; Metz, B.; Behrendt, A.; Harms, K. *J. Organomet. Chem.* **1994**, *481*, 153.

(2) (a) Hendrickson, D. N. In *Magneto-Structural Correlations in Exchange Coupled Systems*; Willet, R. D., Gatteschi, D., Kahn, O., Eds.; NATO Advanced Study Institute Series; Reidel: Dordrecht, The Netherlands, 1985; pp 523–544. (b) See ref 5 for leading references.

(3) Coffman, R. E.; Buettner, G. R. *J. Phys. Chem.* **1979**, *83*, 2387, 2392.

(4) (a) Elschenbroich, Ch.; Heikenfeld, G.; Wünsch, M.; Massa, W.; Baum, G. *Angew. Chem., Int. Ed. Engl.* **1988**, *27*, 414. (b) Metz, B. Ph.D. Dissertation, Marburg, 1992.

(5) Elschenbroich, Ch.; Bretschneider-Hurley, A.; Hurley, J.; Massa, W.; Wocadlo, S.; Pebler, J.; Reijerse, E. *Inorg. Chem.* **1993**, *32*, 5421.

0276-7333/94/2313-5072$04.50/0 

**Chart 1**

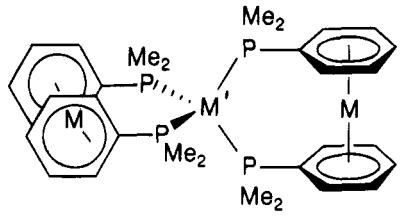

| M′ | M | V | Cr |
|---|---|---|---|
| Ni | | 1 | 4 |
| Pt | | 2 | 5 |
| CoH | | 3 | 6 |

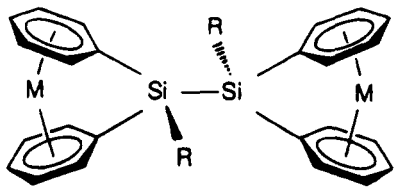

| M | V | Cr |
|---|---|---|
| | 7 | 8 |

**Scheme 1**

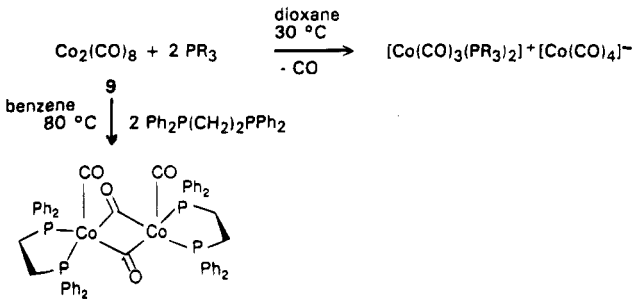

Besides an EPR study of magnetic exchange in the biradicals containing $V^0$ and $Cr^+$ as central metals, cyclic voltammetry (CV) will also be applied to the tetranuclear complexes in a search for redox splitting, which would be another manifestation of weak interaction between the terminal bis(arene)metal units.

## Results and Discussion

**Synthesis and Structure.** Reactions of $Co_2(CO)_8$ with organophosphanes are frequently accompanied by disproportionation particularly if carried out in polar solvents at ambient temperature.[6] This also applies to ditertiary chelating phosphanes.[7] At higher temperatures and in nonpolar media formation of molecules containing $Co_2(CO)_4$ bridges is favored (Scheme 1).[8a]

(6) Hieber, W.; Freyer, F. *Chem. Ber.* **1960**, *93*, 462.
(7) Manning, A. R. *J. Chem. Soc. A* **1968**, 1135.
(8) (a) Manning, A. R.; Thornhill, D. J. *J. Chem. Soc., Dalton Trans.* **1973**, 2086. (b) Mirza, H. A.; Vittal, J.; Puddephat, R. J.; Frampton, C. S.; Manojlovic-Muir, L.; Xia, W.; Hill, R. H. *Organometallics* **1993**, *12*, 2767.

**Table 1. Experimental Parameters of the X-ray Diffraction Study of 14**

| | |
|---|---|
| formula | $C_{36}H_{44}Co_2O_4P_4V_2$ |
| formula wt | 884.38 |
| *a* | 1465.2(3) pm |
| *b* | 1696.5(3) pm |
| *c* | 1571.1(3) pm |
| β | 112.29(2)° |
| *V* | 3613(1) × $10^6$ $pm^3$ |
| *Z* | 4 |
| density (calcd) | 1.625 $g/cm^3$ |
| cryst syst | monoclinic |
| space group | $P2_1/c$ (No. 14[a]) |
| temp | 20 °C |
| no. of reflns for the determination of the cell constants | 25 |
| 2Θ scan range | 4−50° |
| scan type | ω-scan |
| scan width | (1.3 + 0.35 tan Θ)° |
| no. of data collected | 8875 |
| unique data | 6289 |
| obsd data ($F_o > 4\sigma F_o$) | 2921 |
| linear abs coeff ($\mu_{Mo\ K\alpha}$) | 16.2 $cm^{-1}$ |
| $R = \Sigma\|\|F_o\| - \|F_c\|\|/\Sigma\|F_o\|$ | 0.058 |
| $R_w = [\Sigma(\|F_o\| - \|F_c\|)^2/\Sigma w\|F_o\|^2]^{1/2}$ $w = 1/[\sigma^2(F_o^2) + 0.0001F_o^2]$ | 0.045 |
| max/min residual electron density (e/$pm^3$ × $10^6$) | 0.69/−0.64 |

[a] *International Tables for Crystallography*, 2nd ed.; Kluwer Academic Publishers: Dordrecht, 1989.

If cobalt(II) chloride is reduced by $Na[BH_4]$ in the presence of DMPM (= $Me_2PCH_2PMe_2$), the chelating diphosphane engages in A-frame coordination, $[Co_2(CO)_2(\mu\text{-}CO)_2(\mu\text{-DMPM})_2]$ being obtained.[8b] Thus, in order to effect nonbridging coordination, we first treated bis((dimethylphosphano)-$\eta^6$-benzene)chromium, **13**,[4] with $Co_2(CO)_8$ in boiling toluene. However, as inferred from IR spectroscopic evidence pointing to the presence of $Co(CO)_4^-$ units, disproportionation had taken place. We therefore resorted to bis($\eta^2,\eta^{2\prime}$-bicyclo[2.2]hepta-2,5-diene)tetracarbonyldicobalt **11**[9] as a source for the $Co_2(CO)_4$ bridge.

The sparingly soluble products **14** (reddish brown) and **15** (ochre) may be recrystallized from toluene to yield crystals suitable for X-ray diffraction. The structure of the vanadium complex **14** is shown in Figure 1. Experimental data for the crystal structure determination, fractional coordinates, and selected bond lengths and bond angles are listed in Tables 1, 2, and 3, respectively. The rod-shaped molecules in the crystal form parallel strands which are composed of the two enantiomers. The $Co_2(CO)_4$ unit contains two bridging and two terminal CO ligands which leads to a butterfly structure with an interplanar angle of 117°. Compared with the complexes **9** (252.4 pm[10]) and **10** (255.2 pm[4b]), the Co−Co bond distance is significantly shorter in **6** (247.1 pm). The individual sandwich units in **14** display only very slight tilting of the ring plains (angle 4°), the conformation of the $\eta^6$-arenes is staggered, and the disposition of the axial methyl groups $C(10)H_3$ and $C(12)H_3$ as well as $C(13)H_3$ and $C(15)H_3$ is antiperiplanar. Interestingly, in the complex **4** the latter orientation is synperiplanar.[4a] Important structural aspects with regard to the discussion of intramolecular communication are the angle between the terminal sandwich axes (55.3°) and the V···V distance (1094.2 pm). A very similar structure most likely pertains for the

(9) Behrens, H.; Aquila, W. *Z. Anorg. Allg. Chem.* **1967**, *356*, 8.
(10) Summar, G. G.; Klug, H. P.; Alexander, L. E. *Acta Crystallogr.* **1964**, *17*, 732.

**Scheme 2**

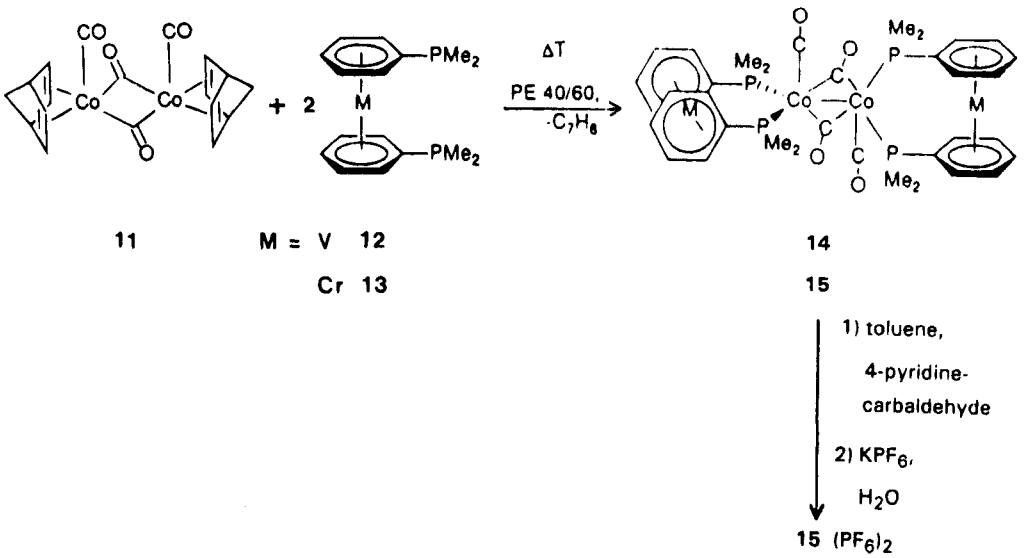


chromium analog **15**. In this case, additional information concerning the dynamic behavior in fluid solution is available from nuclear magnetic resonance. As inferred from the data reported in the Experimental Section, the $^1$H- and $^{13}$C-NMR spectra of the tetranuclear complex **15** are much simpler than the structure in the crystal would suggest. For example, in such a static structure all 20 arene protons should be inequivalent. Equivalence of the two sandwich units may be effected by a process which exchanges bridging and terminal CO ligands in the $Co_2(CO)_4$ unit.[11] Furthermore, the observation that all the ortho, the meta, and the para positions as well as the methyl groups, respectively, are isochronic may be rationalized by cycloreversion of the P–Co–P links as depicted in Figure 2. This type of flexibility of an interannular link, which for **15** is fast on the NMR time scale even at 173 K, is a common phenomenon in the metallocenophane[12] as well as in the metallocyclophane[13] series.

**Electrochemistry.** For the tetranuclear complexes **14** and **15** is a rich redox chemistry may be envisaged since both the central $Co_2(CO)_4$- and the terminal sandwich units can undergo electron-transfer processes. The redox behavior of the species $C_{12}H_{12}M$ (M = V, Cr) has recently been described,[14] and that of the reference compound **10** has also been the subject of detailed investigation.[4b] The most important findings emerging from the latter study are a reversible redox couple $\mathbf{10}^{+/0}$

(11) Lissic, E. C.; Hanson, B. E. *Inorg. Chem.* **1986**, *25*, 812.
(12) Abel, E. W.; Orrell, K. G. *Progr. Inorg. Chem.* **1984**, *32*, 1. Abel, E. W.; Long, N. J.; Orrell, K. G.; Osborne, A. G.; Sik, V.; Bates, P. A.; Hursthouse, M. B. *J. Organomet. Chem.* **1989**, *367*, 275. Herberhold, M.; Leitner, P. *J. Organomet. Chem.* **1991**, *411*, 232 for leading references.
(13) By *metallocyclophane* we designate bis(arene)metal complexes bearing interannular bridges (compare *metallocenophane*; Mueller-Westerhoff, U. T. *Angew. Chem., Int. Ed. Engl.* **1986**, *25*, 702). In *homometallocyclophanes* the bridges are formed from C units exclusively, in *heterometallocyclophanes* they may also contain other main-group or transition elements in their backbone. Cycloreversion: Burdorf, H.; Elschenbroich, Ch. *Z. Naturforsch.* **1981**, *36b*, 94. Elschenbroich, Ch.; Burdorf, H.; Burdorf, H.; Mahrwald, D.; Metz, B. *Z. Naturforsch.* **1992**, *47b*, 1157. Elschenbroich, Ch.; Sebbach, J.; Metz, B.; Heikenfeld, G. *J. Organomet. Chem.* **1992**, *426*, 173. Reference 4.
(14) Elschenbroich, Ch.; Bilger, E.; Metz, B. *Organometallics* **1991**, *10*, 2823.
(15) Behrens, H.; Aquila, W. *Z. Anorg. Allg. Chem.* **1967**, *356*, 8.
(16) Flanagan, J. B.; Margel, S.; Bard, A. J.; Anson, F. C. *J. Am. Chem. Soc.* **1978**, *100*, 4248.

**Table 2. Atomic Coordinates and Isotropical Equivalent Thermal Parameters ($10^{-22}$ m$^2$) of the Non-Hydrogen Atoms in 14**

| atom | *x* | *y* | *z* | $U_{eq}$ |
|---|---|---|---|---|
| Co1 | 0.7087(1) | −0.01936(7) | 0.2550(1) | 2.52(4) |
| Co2 | 0.7927(1) | −0.14318(7) | 0.2412(1) | 2.71(4) |
| V1 | 0.7039(2) | 0.2382(1) | 0.2605(1) | 3.73(6) |
| V2 | 0.7944(1) | −0.4021(1) | 0.2640(1) | 3.92(7) |
| P1 | 0.7168(2) | 0.0619(2) | 0.1461(2) | 2.7(1) |
| P2 | 0.7190(2) | 0.0517(2) | 0.3740(2) | 3.1(1) |
| P3 | 0.6806(2) | −0.2259(2) | 0.1470(2) | 3.0(1) |
| P4 | 0.9022(3) | −0.2126(2) | 0.3477(2) | 3.2(1) |
| O1 | 0.9240(5) | −0.0122(4) | 0.3334(5) | 4.5(3) |
| O2 | 0.6689(5) | −0.1522(4) | 0.3509(4) | 4.1(3) |
| O3 | 0.4954(5) | −0.0311(4) | 0.1796(5) | 5.4(3) |
| O4 | 0.8982(6) | −0.1278(5) | 0.1177(5) | 7.5(4) |
| C1 | 0.8469(8) | −0.0425(5) | 0.2959(7) | 3.1(4) |
| C2 | 0.7061(7) | −0.1194(6) | 0.3060(6) | 3.5(4) |
| C3 | 0.5800(8) | −0.0264(6) | 0.2054(6) | 2.8(4) |
| C4 | 0.8559(8) | −0.1319(5) | 0.1653(7) | 4.3(4) |
| C5 | 0.6685(7) | 0.1595(5) | 0.1425(6) | 2.3(3) |
| C6 | 0.7531(8) | 0.1549(6) | 0.3756(6) | 3.2(4) |
| C7 | 0.6719(7) | −0.3247(5) | 0.1866(7) | 3.2(4) |
| C8 | 0.9104(8) | −0.3178(6) | 0.3250(7) | 3.7(4) |
| C9 | 0.6468(8) | 0.0256(6) | 0.0315(6) | 5.0(4) |
| C10 | 0.8338(7) | 0.0796(6) | 0.1358(6) | 4.4(4) |
| C11 | 0.8060(8) | 0.0191(6) | 0.4844(5) | 5.0(4) |
| C12 | 0.6055(7) | 0.0531(6) | 0.3960(6) | 5.2(4) |
| C13 | 0.6894(8) | −0.2412(6) | 0.0352(6) | 5.2(4) |
| C14 | 0.5497(7) | −0.1988(6) | 0.1070(6) | 4.3(4) |
| C15 | 0.9020(8) | −0.2085(7) | 0.4622(6) | 6.0(5) |
| C16 | 1.0289(7) | −0.1837(6) | 0.3705(7) | 4.9(4) |
| C51 | 0.7117(8) | 0.2299(6) | 0.1239(6) | 3.7(4) |
| C52 | 0.6759(9) | 0.3044(6) | 0.1332(7) | 4.6(4) |
| C53 | 0.5926(8) | 0.3133(6) | 0.1562(6) | 4.1(4) |
| C54 | 0.5460(8) | 0.2453(7) | 0.1712(6) | 4.4(4) |
| C55 | 0.5846(7) | 0.1696(6) | 0.1650(6) | 3.0(4) |
| C61 | 0.7000(8) | 0.2180(6) | 0.3968(6) | 4.5(4) |
| C62 | 0.727(1) | 0.2981(7) | 0.3915(7) | 5.7(5) |
| C63 | 0.805(1) | 0.3148(6) | 0.3666(7) | 5.6(5) |
| C64 | 0.8602(8) | 0.2539(7) | 0.3470(7) | 4.5(4) |
| C65 | 0.8337(8) | 0.1744(6) | 0.3524(6) | 3.5(4) |
| C71 | 0.6682(8) | −0.3938(7) | 0.1343(8) | 4.9(5) |
| C72 | 0.6661(8) | −0.4678(6) | 0.1693(9) | 5.6(5) |
| C73 | 0.6721(8) | −0.4773(7) | 0.2615(9) | 5.8(5) |
| C74 | 0.6747(8) | 0.4104(7) | 0.3147(8) | 5.7(5) |
| C75 | 0.6766(7) | −0.3345(6) | 0.2794(7) | 3.7(4) |
| C81 | 0.9082(7) | −0.3399(6) | 0.2373(7) | 4.1(4) |
| C82 | 0.9145(7) | −0.4186(6) | 0.2136(8) | 5.0(5) |
| C83 | 0.9168(9) | −0.4785(7) | 0.276(1) | 6.4(5) |
| C84 | 0.9245(9) | −0.4583(7) | 0.3683(9) | 7.0(6) |
| C85 | 0.9210(7) | −0.3787(6) | 0.3918(7) | 4.5(4) |

**Table 3. Selected Bond Lengths (pm) and Angles (deg) for 14**

| | | | | | |
|---|---|---|---|---|---|
| Co1–Co2 | 247.1(2) | Co1–P1 | 223.5(3) | V1–C5 | 218.2(9) |
| Co1–P2 | 218.2(3) | Co2–P3 | 225.0(3) | V1–C51 | 220(1) |
| Co2–P4 | 218.2(3) | Co1–C1 | 192(1) | V1–C52 | 219(1) |
| Co1–C2 | 188.4(9) | Co1–C3 | 175(1) | V1–C53 | 222(1) |
| Co2–C1 | 192.6(9) | Co2–C2 | 194(1) | V1–C54 | 221(1) |
| Co2–C4 | 177(1) | O1–C1 | 118(1) | V1–C55 | 216(1) |
| O2–C2 | 118(1) | O3–C3 | 115(1) | V1–C6 | 219.0(9) |
| O4–C4 | 114(2) | P1–C5 | 179.2(9) | V1–C61 | 219(1) |
| P1–C9 | 180.9(9) | P1–C10 | 181(1) | V1–C62 | 220(1) |
| P2–C6 | 182(1) | P2–C11 | 180.7(9) | V1–C63 | 219(1) |
| P2–C12 | 182(1) | P3–C7 | 181(1) | V1–C64 | 219(1) |
| P3–C13 | 183(1) | P3–C14 | 184(1) | V1–C65 | 219(1) |
| P4–C8 | 183(1) | P4–C15 | 180(1) | V2–C7 | 219(1) |
| P4–C16 | 182(1) | | | V2–C71 | 218(1) |
| | | | | V2–C72 | 221(1) |
| | | | | V2–C73 | 219(1) |
| | | | | V2–C74 | 219(1) |
| | | | | V2–C75 | 216(1) |
| | | | | V2–C8 | 215(1) |
| | | | | V2–C81 | 215(1) |
| | | | | V2–C82 | 221(1) |
| | | | | V2–C83 | 216(1) |
| | | | | V2–C84 | 220(1) |
| | | | | V2–C85 | 219(1) |

| | | | |
|---|---|---|---|
| P1–Co1–P2 | 107.9(1) | P3–Co2–C1 | 157.3(3) |
| P3–Co2–P4 | 107.4(1) | P3–Co2–C2 | 90.6(3) |
| Co1–C1–Co2 | 80.0(4) | P3–Co2–C4 | 93.3(4) |
| Co1–C2–Co2 | 80.4(4) | P4–Co2–C1 | 94.6(3) |
| P1–Co1–C1 | 91.6(3) | P4–Co2–C2 | 98.2(3) |
| P1–Co1–C2 | 153.8(3) | P4–Co2–C4 | 98.6(4) |
| P1–Co1–C3 | 93.6(3) | C1–Co2–C2 | 80.3(5) |
| P2–Co1–C1 | 96.0(3) | C1–Co2–C4 | 89.0(5) |
| P2–Co1–C2 | 98.0(3) | C2–Co2–C4 | 160.7(4) |
| P2–Co1–C3 | 97.6(3) | Co1–P1–C5 | 117.3(3) |
| C1–Co1–C2 | 82.1(4) | Co1–P2–C6 | 118.2(3) |
| C1–Co1–C3 | 163.2(4) | Co2–P3–C7 | 119.2(3) |
| C2–Co1–C3 | 86.3(5) | Co2–P4–C8 | 117.8(3) |
| Co1–C1–O1 | 140.3(8) | | |
| Co2–C1–O1 | 139.7(9) | | |
| Co1–C2–O2 | 140.1(8) | | |
| Co2–C2–O2 | 139.5(8) | | |

($E_{1/2}$ = −0.20 V), oxidative cleavage of the Co–Co bond at more anodic potential ($E_{pa}$ = +0.65 V), and reductive cleavage at $E_{pc}$ = −2.32 V. The latter process has been performed previously on a preparative scale using sodium amalgam as a reductant. The redox properties of dinuclear **10** aid in the interpretation of the electrochemistry of **14** and **15**. Cyclovoltammetric traces for **14** and **15** are depicted in Figures 3–5, where the parameters are also given. Our interpretation of the course of electrochemical events for **14** and **15** is given in Scheme 3.

The simpler behavior of chromium complex **15** will be treated first. As expected from a comparison of the redox properties of **10** and **13**, the first oxidation step involves the terminal sandwich units. Compared to the free organometallic ligand ($Me_2P$-$\eta^6$-$C_6H_5)_2Cr$, **13** ($E_{1/2}^{0/+}$ = −0.57 V[4]), the redox potential of **13** as a part of the molecule **15** shows a slight anodic shift which stems from the electron-withdrawing properties of the bridging $Co_2(CO)_4$ unit. The dication $\mathbf{15}^{2+}$ can also be prepared via chemical oxidation by 4-pyridinecarboxaldehyde and isolated as the hexafluorophosphate salt. The infrared data for **15**$(PF_6)_2$ denote that oxidation has occurred at the terminal sandwich moieties since the carbonyl stretching frequencies experience only a moderate shift to higher wavenumbers. This argument rests on a comparison with the IR data of **10**$(PF_6)$. Whereas in DME solvent no redox splitting is discernible, the cyclovoltammogram of the salt **15**$(PF_6)_2$ in $CH_2Cl_2$ points to a difference between the potentials of two consecutive electron transfers, $Cr^{+/0}$ (Figure 5). The redox-splitting $\Delta E_{1/2}$ emerges more clearly from differential pulse voltammetry (DPV) performed in **15**$(PF_6)_2$. From the cyclovoltammogram, on the basis of working curves,[17] a value of $\Delta E_{1/2} \approx 100$ mV may be estimated. DPV yields the value $\Delta E_{1/2}$ = 90 mV. The third electron-transfer step, from a consideration of the peak currents, involves only one of the two cobalt atoms. This assignment was corroborated by chronoamperometric measurements, which yielded the ratio $I_{pa}(\mathbf{15}^{2+/0})$:$I_{pa}(\mathbf{15}^{3+/2+})$ = 2:1. Contrary to the behavior of the dinuclear cobalt complex **10**, for tetranuclear $\mathbf{15}^{2+}$ this step is reversible. Apparently for $\mathbf{15}^{3+}$ stabilization by electron delocalization is more effective than for **10**. A strong interaction between the $\mathbf{13}^{\bullet+}$ terminal units and the $Co_2(CO)_4$ bridge is also suggested by the pronounced anodic shift of +350 mV that the couple $Co_2(CO)_4^{+/0}$ experiences in $\mathbf{15}^{2+}$ compared to **10**. The fourth oxidation step for **15** is irreversible, as is reduction, which is signalized by an irreversible step at $E_{pc}$ = −2.59 V. As in the case of **10**, cleavage of the $Co_2(CO)_4$ unit probably takes place at this potential.

For the divanadium analog **14** as well, primary oxidation occurs at the terminal bis(arene)metal units and in the cyclovoltammogram displays a redox splitting of a magnitude similar to that of **15**. From the peak separation $\Delta E_p$ = 110 mV, and the difference $E_{pa} - E_{pa/2}$ = 90 mV working curves[17] yield the redox-splitting $\Delta E_{1/2} = E_{1/2}(\mathbf{14}^{2+/+}) - E_{1/2}(\mathbf{14}^{+/0}) \approx 80$ mV. Unfortunately, we were not able to obtain satisfactory DPV response for **14**. If, starting from the initial limits $-1.0 < E < +0.2$ V, the scan range is gradually extended in the anodic direction, oxidation of the central unit $Co_2(CO)_4$ is observed. However, as opposed to the dichromium complex **15**, this process is irreversible for the divanadium species **14**. No plausible explanation is available for this diverging behavior. That the second oxidation step for **14** occurs at a bis(arene)vanadium unit is highly unlikely in view of its position on the potential scale, since the irreversible step $(C_6H_6)_2V^{2+/+}$ is known to proceed at $E_{pa}$ = 0.24 V,[14] and for the bis(arene)-vanadium moiety, present in the dication $\mathbf{14}^{2+}$, a much more anodic peak potential would be expected. While irreversibility of the processes leading to a higher oxidation and reduction stages of the complexes **14** and **15** precludes detailed discussion, the redox splitting of the reversible primary redox processes which yield the mono- and dications is remarkable in view of the fact that the terminal redox centers are separated by a distance of more than 1000 pm. It would be premature, however, to conclude that this distance defines the limit beyond which intramolecular interations of redox centers become unobservable by electrochemical methods, because there may be spacers different from the (-$PMe_2)_2$-$Co_2(CO)_4(PMe_2^-)_2$ bridge that may sustain redox communication over even larger distances.

**EPR Spectroscopy.** Whereas the measurement of magnetic susceptibility as a method for determining the exchange coupling constant $J$ fails for $J < 1$ cm$^{-1}$, it is for this region of very weak interaction that electron paramagnetic resonance, in particular the inspection of the hyperfine coupling pattern, steps in. The EPR spectrum of the bisvanadium complex **14** is shown in

(17) Richardson, D. E.; Taube, H. *Inorg. Chem.* **1981**, *20*, 1278.

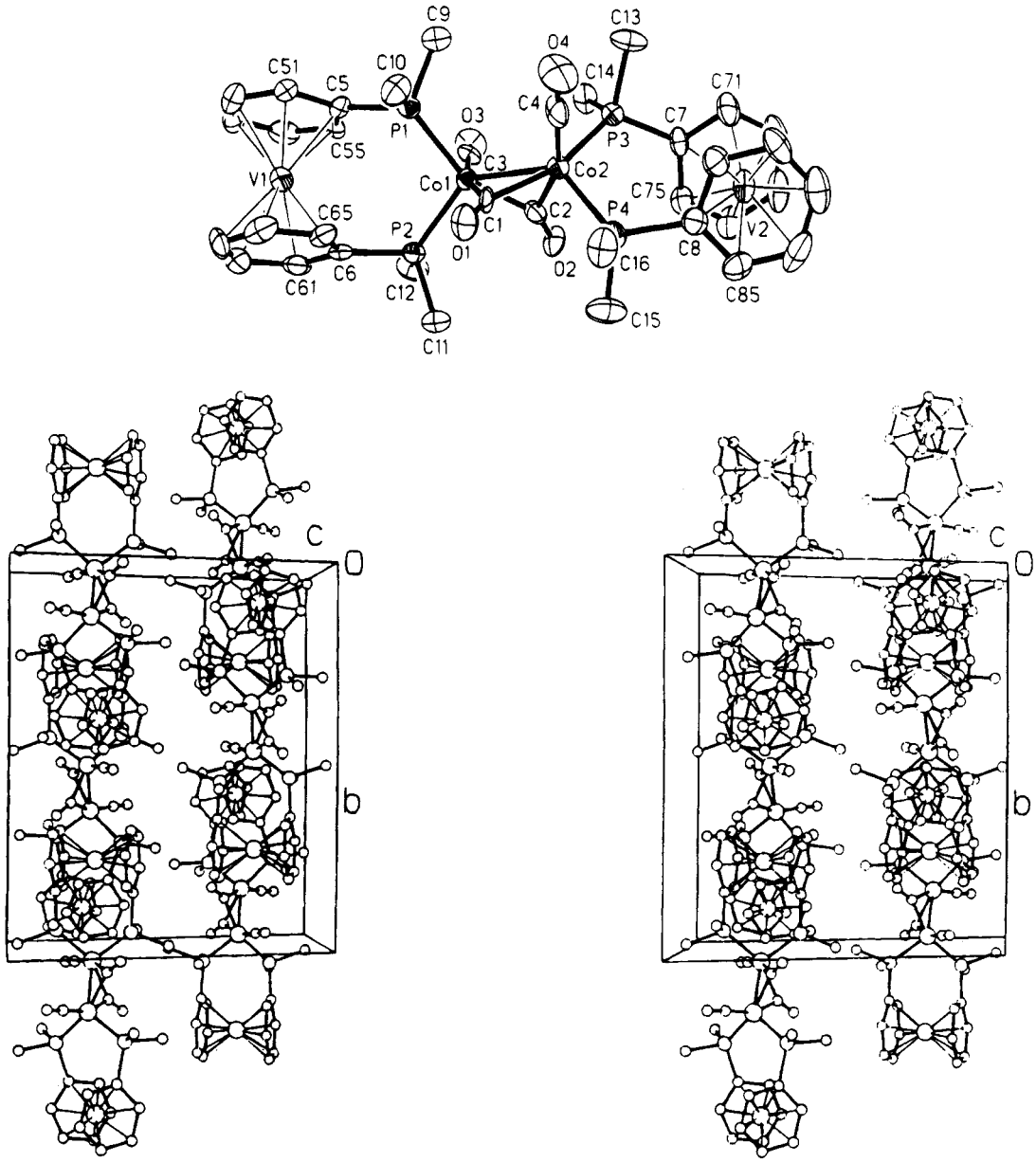


**Figure 1.** Molecular structure (top) and unit cell (bottom) of complex **14**.

Figure 5. The fairly complicated, irregular pattern immediately suggests that exchange coupling $J$ and hyperfine coupling $a(^{51}V)$ must be of similar magnitude, i.e., that an intermediate exchange situation prevails. This qualitative conclusion is supported by spectral simulation in which fair agreement with the experimental trace is achieved with $J = -0.078$ cm$^{-1}$, while for the mononuclear complex **12**, $a(^{51}V) = 0.0063$ cm$^{-1}$. Replacing the spacer >Si(Ph)-Si(Ph)< by the unit (-$PMe_2$)$Co_2(CO)_4$($PMe_2$-)$_2$ has the effect of increasing the intermetallic distance V···V from ≈760 pm (**7**)[5] to 1094 pm (**14**) with an attendant decrease of exchange coupling from $J$(**7**) = −0.48 cm$^{-1}$ to $J$(**14**) = −0.078 cm$^{-1}$. Interestingly, despite the magnetic moment ($I(^{59}Co)$ = 7/2, 100%), the $^{59}$Co nuclei in the tetranuclear complex **14** are EPR-silent, which raises questions concerning the mechanism of the exchange coupling. In essence, they concern the seemingly paradoxical situation that both unpaired electrons interact with both vanadium nuclei, but there is no evidence for spin density on the bridge.[18]

The diradical dication **15**$^{\bullet\bullet 2+}$, which is isoelectronic to **14**$^{\bullet}$, in fluid solution yields only a broad signal void of proton hyperfine structure. Possibly, intramolecular exchange broadening is responsible for this observation, being more effective in eliminating resolution of individual hyperfine components in the case of small coupling constants $a(^1H$, **15**) compared to the large values for $a(^{51}V$, **14**). The EPR spectra of **14**$^{\bullet}$ and **15**$^{\bullet\bullet 2+}$ also differ significantly in rigid solution. The complex **14** yields a spectrum displaying rich $^{51}$V hyperfine structure. An analysis of this spectrum would have to consider a large number of parameters, namely, the components of the zero-field splitting, $g$, and hyperfine tensors, which at present is impractical. A half-field signal ($\Delta M_s = 2$) is not observed for **14**$^{\bullet}$, which does

(18) A discussion of the alternative mechanisms—"direct" (metal orbital overlap) or "indirect" (superexchange)—will be based on additional experiments currently in progress. They involve a comparison of the temperature dependence of the exchange coupling constant $J$ for closed (rigid) and open (flexible) analogs of **1** and **4**. In this way it should become possible to differentiate between through-space and through-bond processes.

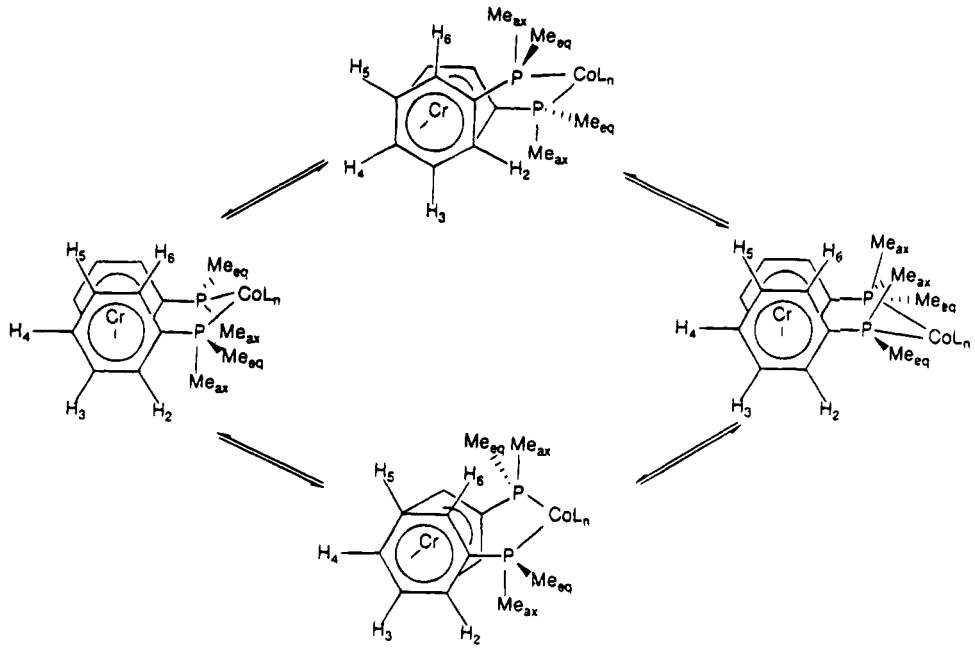

**Figure 2.** Cycloreversion of the interannular bridge in the tetranuclear complex **15**.

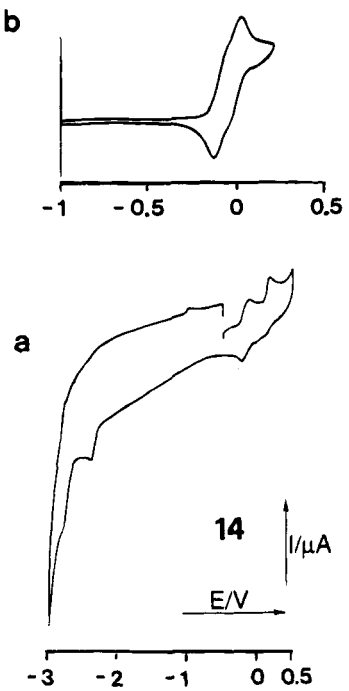


**Figure 3.** Cyclic voltammogram of **14** at −50 °C, DME/0.1 M TBAP *vs* SCE. $E_{pc} = -2.82$ V (irrev); $E_{pc} = -2.47$ V (irrev); $E_{1/2} = -0.22$ V, $r = i_a/i_c \approx 1$; $E_{1/2} = -0.14$ V, $r \approx 1$; $E_{pa} = 0.18$ V (irrev); $E_{pa} = 0.67$ V (irrev). (a) Survey, $-3.0 < E < 0.5$ V, 200 mV/s. (b) Limited scan range, $-1.0 < E < 0.2$ V, 20 mV/s.

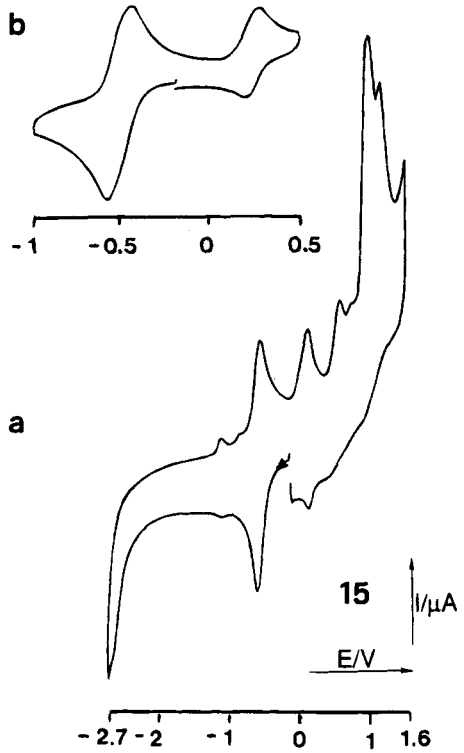


**Figure 4.** Cyclic voltammogram of **15** at −50 °C, DME/TBAP *vs* SCE. $E_{pc} = -2.59$ V (irrev); $E_{1/2} = -0.53$ V, $\Delta E_p = 90$ mV, $r = 1$, $n = 2$; $E_{1/2} = 0.24$ V, $\Delta E_p = 92$ mV, $r = 1.1$; $E_{pa} = 0.62$ V (irrev); $E_{pa} = 1.05$ V (irrev). (a) Survey, $-2.7 < E < 1.6$ V. (b) Limited scan range, $-1.0 < E < 0.5$ V, 200 mV/s.

not come as a surprise in view of the large interspin distance and the fact that total intensity is distributed over 15 $^{51}$V hyperfine components. Conversely, the lack of hyperfine resolution simplifies the spectrum of the dichromium complex **15**$^{\bullet\bullet 2+}$ in rigid solution (Figure 6), allowing observation of the $\Delta M_s = 2$ transition at the $2.5 \times 10^{-4}$ relative intensity of the $\Delta M_s = 1$ signal. Furthermore, in the $\Delta M_s = 1$ region, the central line is accompanied by two signals which are separated by 5.23 mT. While the overall shape of the $\Delta M_s = 1$ signal does not display all the features expected for a nonaxial species in its triplet state (the $D + 3E$ and $D - 3E$ pairs of lines are not resolved), the outer lines may be assigned to the $Z$ components of the $\Delta M_s = 1$ transition (separation $2D = 52 \times 10^{-4}$ cm$^{-1}$). If one proceeds to calculate the interspin distance $r$ from this separation according to the relation $r = (3g\beta/2D)^{1/3}$,[19] a value of

(19) Eaton, S. S.; More, K. M.; Savant, B. M.; Eaton, G. R. *J. Am. Chem. Soc.* **1983**, *105*, 6560.

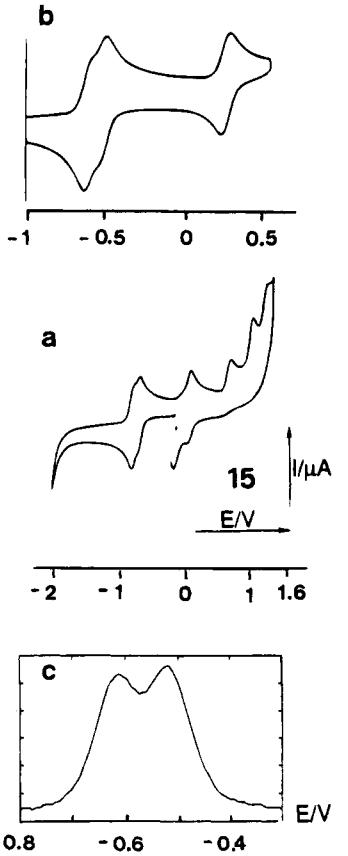


**Figure 5.** Cyclic voltammogram of **15** at 25 °C, $CH_2Cl_2$/$(n\text{-}Bu)_4NPF_6$ *vs* SCE. $E_{1/2} = -0.63$ V; $E_{1/2} = -0.52$ V, $\Delta E_p$-(2+/0) = 155 mV; $E_{1/2} = 0.23$ V, $\Delta E_p = 65$ mV, $r = 1.0$; $E_{pa} = 0.91$ V; $E_{pa} = 1.27$ V; $E_{pa} = 1.53$ V. (a) Survey, $-2.0 < E < 1.5$ V, 200 mV/s. (b) Limited scan range, $-1.0 < E < 0.5$, 50 mV/s. (c) Differential pulse voltammogram, $-0.8 < E < 0.3$ V, 10 mV/s; scan increment 2 mV; step drop time 0.2 s; pulse height 20 mV; pulse width 40 ms.

1002 pm is obtained, which falls considerably short of the distance inferred for **14** from the X-ray structure determination. In view of the poor resolution of the $\Delta M_s = 1$ signal, not too much weight should be put on this divergence. If it is assumed that the numerical value of the parameter has been extracted correctly from the spectrum, the inconsistency would signalize that for $\mathbf{15}^{\bullet\bullet 2+}$ the point-dipole approximation is not strictly applicable. This could derive from a direct (through-space) $Cr^{\bullet+}\cdots Co-Co\cdots Cr^{\bullet+}$ interaction which fakes a shorter distance between the terminal paramagnetic bis(arene)metal units. It must be admitted, however, that in the case of the dication $\mathbf{4}^{\bullet\bullet 2+}$, which contains the configuration $Cr^{\bullet+}\cdots Ni\cdots Cr^{\bullet+}$ and orthogonal sandwich units, application of the point-dipole model for the calculation of the interchromium distance worked very well.[4] Thus, the reliability of intermetallic distances obtained from the rigid solution EPR spectra of organometallic biradicals is limited by the lack of independent evidence concerning the detailed mechanism of spin–spin interaction.[20]

(20) For a discussion of the applicability of the point-dipole approximation, see: Samuel, E.; Harrod, J. F.; Gourier, D.; Dromzee, Y.; Robert, F.; Jeannin, Y. *Inorg. Chem.* **1992**, *31*, 3252.

(21) Program MAGRES: Keijsers, C. P.; Reijerse, E. J.; Stam, P.; Dumont, M. F.; Gribnau, M. C. M. *J. Chem. Soc., Faraday Trans. 1* **1987**, *83*, 3613.

**Scheme 3**

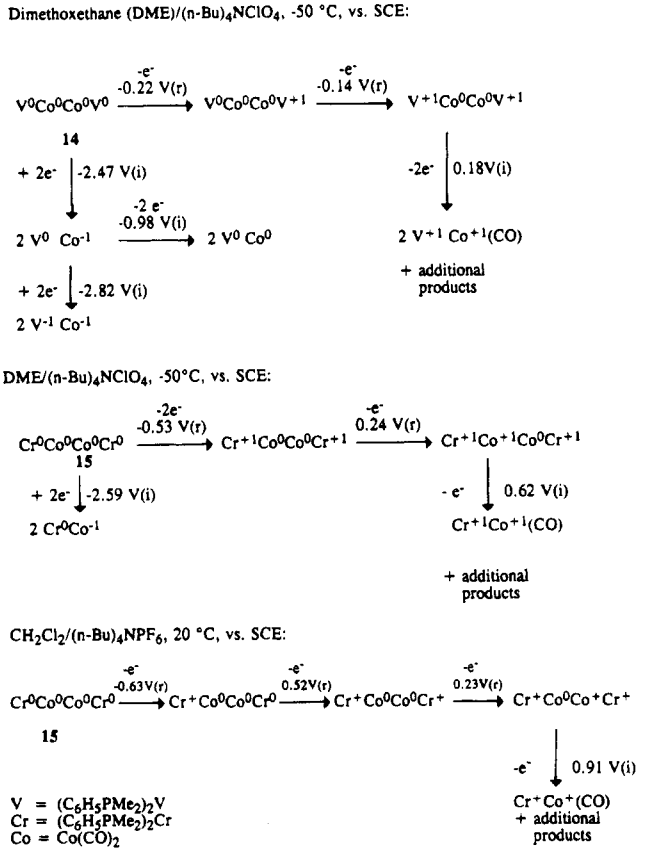


## Experimental Section

Synthetic and spectroscopic work was carried out under an atmosphere of dinitrogen; cyclic voltammetry was conducted under argon. The following instruments were used: Bruker AC-300 and AM-400 (NMR); Varian EE 12 (EPR, X-band); Varian MAT CH7A (EI-MS); AMEL Models 552, 568, 563; Nicolet storage oscilloscope 3091; glassy carbon working electrode; Pt wire counter electrode; saturated calomel reference electrode; EG+G (PAR) Model 273; Pt disk working electrode; Pt wire counter electrode; SCE reference electrode; and Electrochemical Analysis Software Model 270 (cyclic voltammetry, differential pulse voltammetry). Measurements were performed in the media dimethoxyethane (DME)/$(n\text{-}Bu)_4NClO_4$, 0.1 M, and methylene chloride/$(n\text{-}Bu)_4NPF_6$, 0.1 M.

**Bis[bis((dimethylphosphano)-$\eta^6$-benzene)vanadium]-bis($\mu$-carbonyl)dicarbonyldicobalt (Co–Co) (14).** Bis($\eta^4$-norbornadiene)dicobalt tetracarbonyl (**11**)[9] (0.27 g, 0.65 mmol) and bis(dimethyl-$\eta^6$-benzene)vanadium (**12**)[22] (0.42 g, 1.29 mmol) are dissolved in 50 mL of petroleum ether, 40/60, and stirred under reflux for 8 h. The brown precipitate is washed with petroleum ether and extracted with 100 mL of boiling toluene. Upon cooling to 6 °C, the complex **14** (0.35 g, 61%) crystallizes as dark-brown cubes. Anal. Calcd for $C_{36}H_{44}O_4P_4Co_2V_2$: C, 48.89; H, 5.02. Found: C, 48.25; H, 4.65. IR(Nujol): $\nu$(CO) 1945 s, 1910 s, 1735 m, 1705 s.

**Bis[bis((dimethylphosphano)-$\eta^6$-benzene)chromium]-bis($\mu$-carbonyl)dicarbonyldicobalt (Co–Co) (15).** The procedure is analogous to that given for **14**. From **11** (0.20 g, 0.48 mmol) and **13**[4] (0.35 g, 1.07 mmol) is obtained **15** (0.27 g, 63%) as reddish brown cubes. Anal. Calcd for $C_{36}H_{44}O_4P_4$-

(22) The complex $(Me_2P\text{-}\eta^6\text{-}C_6H_5)_2V$ (**12**) was prepared in analogy to the synthesis of $(Ph_2P\text{-}\eta^6\text{-}C_6H_5)_2V$: Elschenbroich, Ch.; Stohler, F. *Chimia* **1974**, *28*, 730.

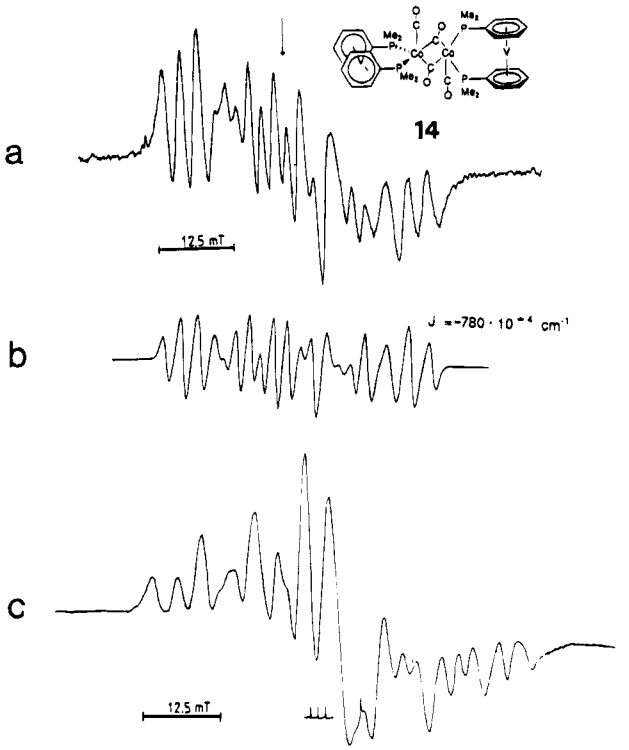


**Figure 6.** EPR spectra of the biradical complex **14**•. (a) Fluid solution (toluene) at 293 K. (b) Stimulated trace.[20] (c) Rigid solution (toluene) at 121 K.

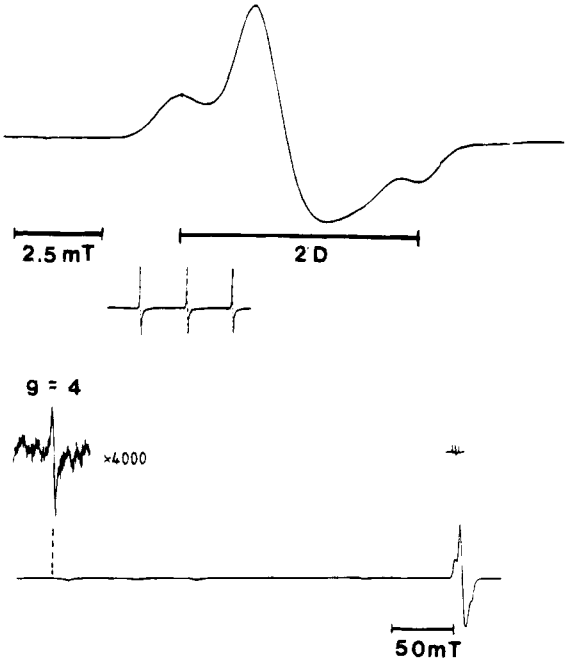


**Figure 7.** EPR spectra of $\mathbf{15}^{\bullet 2+}(PF_6)_2$ in rigid solution ($DMF/CHCl_3$) at 126 K.

$Co_2Cr_2$: C, 48.77, H, 5.01. Found: C, 48.37; H, 5.25. IR(Nujol): ν(CO) 1940 s, 1910 s, 1720 m, 1700 s. $^1$H-NMR ($C_6D_5CD_3$): δ 1.49 ($CH_3$, $^2J(^1H, ^{31}P)$ = 6.9 Hz, 24 H), 4.34 (para, 4 H), 4.45 (meta, 8 H), 4.66 (ortho, 8 H) ppm. $^{13}C\{^1H\}$NMR ($C_6D_5CD_3$): δ 17.5 ($CH_3$), 75.5 (para), 77.9 (meta), 79.6 (ortho) ppm. $^{31}P\{^1H\}$NMR ($C_6D_5CD_3$): δ 12.2 ppm.

**Bis[bis(dimethylphosphano)-η$^6$-benzene)chromium]-bis(μ-carbonyl)dicarbonyldicobalt (Co−Co) bis(hexafluorophosphate) [15(PF$_6$)$_2$].** To a solution of **15** (0.19 g, 0.11 mmol) in 100 mL of toluene at 0 °C are added 20 mL of saturated, aqueous $KPF_6$ solution and 2 mL of 4-pyridinecarboxaldehyde. After the mixture is vigorously stirred for 1 h, the green precipitate is filtered and washed with water, toluene, and diethyl ether. Recrystallization from acetone/diethyl ether yields **15**$(PF_6)_2$ (0.10 g, 77%) as green needles. Anal. Calcd for $C_{36}H_{44}Co_2Cr_2F_{12}P_6$: C, 36.75; H, 3.78. Found: C, 37.01; H, 4.03. IR($CH_2Cl_2$): ν(CO) 1956 s, 1937 s, 1741 m, 1718 m. IR(Nujol): ν(CO) 1965 s, 1935 s, 1750 s, 1740 m.

**Crystal Structure Determination of 14.** A crystal of **14** was mounted in a thin-walled capillary under argon and adjusted on a goniometer head. X-ray intensity data were collected on an Enraf-Nonius CAD4 diffractometer by using an ω-scan with Mo $K_\alpha$ radiation (λ = 71.073 pm, graphite monochromator) at 20 °C. The structure was solved by direct methods and refined by full-matrix least-squares techniques (SHEXLTL-Plus[23]). An extinction correction and a numerical absorption correction ($R_{int}$ = 0.042) were applied to all data. Hydrogen atoms were included by using a riding model with $d$(C−H) = 96 pm and a refined isotropic thermal parameter of $6.1 \cdot 10^{-22}$ m$^2$. Tables for bond lengths, bond angles, and $U_{eq}$ (equivalent isotropic $U$ defined as one-third of the trace of the orthogonalized $U_{ij}$ tensor) were generated with the program PLATON.[24]

**Acknowledgment.** This work was supported by the Deutsche Forschungsgemeinschaft and the Fonds der Chemischen Industrie.

**Supplementary Material Available:** ORTEP drawing and stereoview of the structure of **14** and tables of bond lengths and bond angles, atomic coordinates, and isotropic thermal parameters (11 pages). Ordering information is given on any current masthead page.

OM9403481

(23) Sheldrick, G. M. *SHELXTL-Plus*, Release 4.2 for Siemens R3 Crystallographic Research Systems; Siemens Analytical X-Ray Instruments Inc.: Madison, WI, 1990.
(24) Spek, A. L. PLATON-92; Utrecht, 1992.
(25) Johnson, C. K. *ORTEP*. ORNL-3794; Oak Ridge National Laboratory: Oak Ridge, TN, 1965.